



Sacred Heart
UNIVERSITY

Sacred Heart University
DigitalCommons@SHU

School of Computer Science & Engineering
Faculty Publications

School of Computer Science and Engineering

2019

Electrochemical Amperometric Biosensor Applications of Nanostructured Metal Oxides: A Review

Bünyamin Sahin
Mustafa Kemal University

Tolga Kaya
Sacred Heart University

Follow this and additional works at: https://digitalcommons.sacredheart.edu/computersci_fac



Part of the [Chemistry Commons](#), and the [Computer Sciences Commons](#)

Recommended Citation

Sahin, B., & Kaya, T. (2019). Electrochemical amperometric biosensor applications of nanostructured metal oxides: A review. *Materials Research Express*, 6(4). Doi: 10.1088/2053-1591/aafa95

This Peer-Reviewed Article is brought to you for free and open access by the School of Computer Science and Engineering at DigitalCommons@SHU. It has been accepted for inclusion in School of Computer Science & Engineering Faculty Publications by an authorized administrator of DigitalCommons@SHU. For more information, please contact ferribyp@sacredheart.edu, lysobeyb@sacredheart.edu.

ACCEPTED MANUSCRIPT

Electrochemical amperometric biosensor applications of nanostructured metal oxides: A review

To cite this article before publication: Bunyamin Sahin *et al* 2018 *Mater. Res. Express* in press <https://doi.org/10.1088/2053-1591/aafa95>

Manuscript version: Accepted Manuscript

Accepted Manuscript is “the version of the article accepted for publication including all changes made as a result of the peer review process, and which may also include the addition to the article by IOP Publishing of a header, an article ID, a cover sheet and/or an ‘Accepted Manuscript’ watermark, but excluding any other editing, typesetting or other changes made by IOP Publishing and/or its licensors”

This Accepted Manuscript is © 2018 IOP Publishing Ltd.

During the embargo period (the 12 month period from the publication of the Version of Record of this article), the Accepted Manuscript is fully protected by copyright and cannot be reused or reposted elsewhere.

As the Version of Record of this article is going to be / has been published on a subscription basis, this Accepted Manuscript is available for reuse under a CC BY-NC-ND 3.0 licence after the 12 month embargo period.

After the embargo period, everyone is permitted to use copy and redistribute this article for non-commercial purposes only, provided that they adhere to all the terms of the licence <https://creativecommons.org/licenses/by-nc-nd/3.0>

Although reasonable endeavours have been taken to obtain all necessary permissions from third parties to include their copyrighted content within this article, their full citation and copyright line may not be present in this Accepted Manuscript version. Before using any content from this article, please refer to the Version of Record on IOPscience once published for full citation and copyright details, as permissions will likely be required. All third party content is fully copyright protected, unless specifically stated otherwise in the figure caption in the Version of Record.

View the [article online](#) for updates and enhancements.

Electrochemical Amperometric Biosensor Applications of Nanostructured Metal Oxides: A Review

Bünyamin Sahin^{1, a} and Tolga Kaya²

¹Department of Physics, Faculty of Arts and Sciences, Mustafa Kemal University, Hatay, 31034, Turkey

²Computer Engineering, School of Computing, Sacred Heart University, Fairfield, CT 06515, USA

Abstract

Biological sensors have been extensively investigated during the last few decades. Among the diverse facets of biosensing research, nanostructured metal oxides (NMOs) offer a plethora of potential benefits. In this article, we provide a thorough review on the sensor applications of NMOs such as glucose, cholesterol, urea, and uric acid. A detailed analysis of the literature is presented with organized tables elaborating the fundamental characteristics of sensors including the sensitivity, limit of detection, detection range, and stability parameters such as duration, relative standard deviation, and retention. Further analysis was provided through an innovative way of displaying the sensitivity and linear range of sensors in figures. As the unique properties of NMOs offer potential applications to various research fields, we believe this review is both timely and provides a comprehensive analysis of the current state of NMO applications.

Keywords: Metal oxides, Biosensor, Glucose, Urea, Cholesterol

a) Corresponding Author: Bünyamin Şahin, bsahin@mku.edu.tr

Contents

1. Introduction	0
2. Applications of NMOs in Biosensors	0
2.1. Glucose Sensors	0
2.2. Urea and Uric Acid Sensors	0
2.3. Cholesterol Sensors	0
2.4. Other Sensor Applications	0
3. Conclusion and Future Prospectives	0
References	0

1. Introduction

As the need for portable and low-cost analytical instruments increased, biological sensors have been employed extensively for selective analyte detection [1-3]. Biosensors, in general, require a sensing layer designed to react with a specific biomarker or biomolecule. This sensing information is transformed into either optical, electrochemical, electrical, or other physical signals [4-7]. This article focused specifically on amperometric sensors as a subset of electrical detection of analytes.

In the case of amperometric sensing, current output of the sensor with sensor analyte is measured and used as the parameter for sensing performance. Current values from different concentrations of analyte are gathered to determine the sensitivity of the device. Comparing to other sensing types, amperometric sensing uses only current measurements rather than utilizing sensitive equipment such as optical and electrochemical measurement devices. Current measurements can simply be obtained by using two electrodes to apply voltage and measure current through the device, allowing

1
2
3 a true surface sensitivity measurements particularly for nanostructure based amperometric sensors,
4 which is the focus of this review article.
5
6

7 Nanostructures, contrary to their bulk counterparts, have a high surface-to-volume ratio and surface
8 free energy due to their respective size to volume ratios. This unique property leads to stronger
9 enzyme absorption, which is critical for enzymatic sensors [8,9]. As the size of a particle goes to
10 nano-scale, physical properties of the materials change drastically due to quantum confinement
11 effects [9,10]. Therefore, the conductivity of nanostructures found in nanorods, nanowires,
12 nanotubes, and nanofibers are much higher than their bulk counterparts. The higher conductivity
13 results in an increased signal-to-noise ratio and corresponding sensitivity. The band-gap of a
14 nanostructure structure differs from bulk materials mainly because grains are now essentially
15 defined as a single particle rather than large crystals [10-12]. Nanostructures allow large number
16 of enzyme biomolecules to be immobilized on the electrode surface with increased free energy of
17 nanostructures.
18
19
20
21
22
23
24
25

26 Sensitivity for biosensors is particularly important in clinical diagnostics because giving an
27 accurate reading to clinicians and physicians would be vital. Nanostructures make an excellent
28 candidate as the sensing material in terms of sensitivity for variety of reasons: (1) An increased
29 surface area leads to enhanced sensitivity for particularly small analytes where the size of
30 nanoparticles become comparable to those analytes [13, 14]. (2) Improved direct electron transfer
31 yields an increased sensitivity and an enhanced detection limit [12]. (3) The size of nanostructure
32 particles is close to the Debye length which is known to increase sensor sensitivity [15].
33
34
35
36
37
38

39 While nanostructures can be synthesized using variety of advanced materials, nanostructured metal
40 oxides (NMOs) were chosen as the focus of this review article since NMOs in biosensors has drawn
41 significant attention in the last decade. In the case of NMO materials, the above mentioned
42 advantages of nanostructures directly apply. Furthermore, the surface morphology and the shape
43 of nanostructures can simplify modification of NMO-related fabrication processes. These
44 processes include but not limited to SILAR (Successive Ionic Layer Adsorption and Reaction) [16],
45 chemical bath deposition (CBD) [17], chemical vapor deposition (CVD) [18], sol-gel [19], and
46 pulsed layer deposition (PLD) [20]. This variety of fabrication methods allow easy changes to the
47 nanostructure shape and geometry making NMOs very attractive materials for biosensing devices
48
49
50
51
52
53
54
55 [21].
56
57
58
59
60

1
2
3 The bandgap value of NMOs falls within the semiconducting region, allowing them to be used in
4 sensors [22, 23]. The sensing properties of NMOs depend on their semiconductor type. n-type and
5 p-type semiconductors behave differently in terms of receptor functions, conduction paths, and
6 sensing mechanisms due to different types of majority charge carriers. Common p-type metal oxide
7 semiconductors include copper oxide (CuO), cuprous oxide (Cu₂O), nickel oxide (NiO), cobalt
8 oxide (Co_xO_x), and manganese oxides (Mn_xO_y) whereas n-type NMOs include tin oxide (SnO₂),
9 zinc oxide (ZnO), titanium oxide (TiO₂), and iron oxides (Fe_xO_y) [24, 25]. One of the biggest
10 challenges remaining in the application of NMOs is the high tendency of adhesion and aggregation
11 of NMOs due to high surface energy [26].
12
13
14
15
16
17
18

19 In this review paper, we have focused on particularly glucose, urea and uric acid, and cholesterol
20 sensors that utilize NMOs. We have summarized each sensor in tables by categorizing them with
21 the NMOS types. Furthermore, we devised a method of visual representation of the summarized
22 table using figures where sensitivity and linear range were presented. Each section of the review
23 offers extensive literature review and a quality discussion on different applications and NMOS
24 types.
25
26
27
28
29

30 **2. Applications of NMOs in Biosensors**

31
32 This current review focuses on NMOs that are utilized in electrochemical biosensing applications.
33 We have organized this review by having separate sections for glucose, urea/uric acid, and
34 cholesterol sensors in sections 2.1, 2.2, and 2.3, respectively. Furthermore, we have combined some
35 other types of sensing applications in section 2.4 which included hydrogen peroxide, DNA, and
36 some unconventional sensing approaches. We have summarized the articles in respective tables
37 where we listed their sensing properties such as sensitivity, limit of detection, detection range, and
38 Michaelis–Menten Constant (K_m) value. We have also included stability parameters in tables
39 such as duration, relative standard deviation (RSD), and long term stability. An alternative way of
40 presenting the tables was devised where sensitivity and linear range were plotted.
41
42
43
44
45
46
47
48
49
50
51
52

53 **2.1. Glucose Sensors**

1
2
3 Glucose sensing has been studied since late 1970s in order to help monitor glucose levels of
4 diabetic patients. Most chemical glucose sensing technologies rely on enzymatic reactions in which
5 enzymes catalyze glucose oxide (GOx) generating reactions [27,28]. This method is considered a
6 gold standard but suffers from degraded readings due to pH and temperature changes. Recently,
7 non-enzymatic glucose sensors were developed and metal oxides proved to be one of the promising
8 materials in the use of glucose sensing [29]. Particularly, CuO, ZnO, TiO₂, SnO₂, Cerium Oxide
9 (CeO₂), NiO, and MnO_x have been studied for potential integration into glucose sensors [30-35].
10 Amperometric glucose sensors are mainly characterized through cyclic voltammograms (CVs) and
11 electrochemical impedance spectroscopy (EIS). The main characterization parameter of the
12 amperometric glucose sensors is the sensitivity to the glucose concentration, which is generally
13 given in current change per mM in a square centimeter; $\mu\text{A mM}^{-1} \text{cm}^{-2}$. Sensitivity ranges between
14 1-5000 $\mu\text{A mM}^{-1} \text{cm}^{-2}$. Also, the detection range is one of the important parameters which
15 determines the lower and upper glucose concentrations that the sensor can detect. It is known that
16 the clinical blood glucose levels are between 4.4 mM and 6.6 mM.

17
18
19
20
21
22
23
24
25
26
27
28 CuO stands out among all the other NMOs due to its intrinsic p-type semiconductor property, high
29 stability, capability for electron transfer, and nontoxicity [36,37]. CuO based glucose sensing
30 applications has focused primarily on synthesis and fabrication methods. The main goal is to
31 control the physical properties of CuO nanostructures which directly affect the sensitivity and
32 response/recovery time of glucose analytes. Utilizing Cu foil as the electrode and the substrate, Li
33 et. al. developed flower-like CuO nanostructures for non-enzymatic glucose sensing [38]. The
34 sensitivity for particularly dandelion-like structures reached above 5,000 $\mu\text{A mM}^{-1} \text{cm}^{-2}$ which is
35 much higher than traditional NMO glucose sensors. Additionally, with its wide detection range (5
36 μM to 1.6 mM), the sensor was tested with human serum samples and measurements agreed with
37 hospital-used blood sugar instruments [38]. An enzymatic CuO glucose sensor was fabricated
38 where nanostructured CuO wires, platelets, and spindles were synthesized by using one precursor.
39 Sensor performance was tested by using carbon electrodes as the substrate and resulted in relatively
40 low sensitivity values ($62 \mu\text{A mM}^{-1} \text{cm}^{-2}$) for a limited detection range (1 μM – 80 μM) [39]. Li et.
41 al. produced crystallized leaf-like CuO nanostructures for the development of an amperometric
42 glucose sensor with a sensitivity of $246 \mu\text{A mM}^{-1} \text{cm}^{-2}$ [40]. Although the detection range was
43 relatively narrow (1 μM – 170 μM), sensor responded the human serum levels (up to 40 μM) well
44 and it was stable for 90 days. A wide linear detection range (4 μM to 8 mM) was achieved by Wang
45
46
47
48
49
50
51
52
53
54
55
56
57
58
59
60

1
2
3 et. al. through CuO nanorods and flowers [41]. The sensitivity values for flowers like CuO
4 structures reached up to $709.52 \mu\text{A mM}^{-1} \text{cm}^{-2}$. Kim et. al.'s proposed rose-like CuO nanostructures
5 reached even higher glucose detection range (0.78 μM to 100 mM) with a high sensitivity (4640
6 $\mu\text{A mM}^{-1} \text{cm}^{-2}$) [42]. These structures remained stable as long as 42 days.
7
8
9

10 Cu₂O nanostructures were also used for glucose sensing. Cu₂O has a cubic structure rather than a
11 monoclinic crystal structure as CuO which affects its sensing performances significantly. Khan et.
12 al.'s shuriken-like Cu₂O nanostructures exhibited a 6 decades wide range of sensitivity (0.01 μM
13 to 11.0 mM) with an extremely low detection limit (35 nM) [43]. Moreover, they performed
14 rigorous selectivity analysis of glucose to lactose, fructose, mannose, ascorbic acid, and uric acid,
15 which makes Cu₂O a very promising NMO for glucose sensing.
16
17
18
19
20
21
22
23

24 Zinc oxide (ZnO) is an important member of II-VI group semiconductors. Nanostructured ZnO
25 structures are nontoxic, chemically stable and biocompatible in most cases, which made them
26 attractive for biomedical research, particularly for sensors. An early study on ZnO based glucose
27 sensors explored using ZnO nanocomb structures functionalized with glucose oxidase that
28 exhibited a more than 2 decades of linear range (0.02 mM – 4.5 mM) with a sensitivity of 15.33
29 $\mu\text{A mM}^{-1} \text{cm}^{-2}$ [44]. However, selectivity or stability analysis were not performed. Similarly,
30 glucose oxidase adsorbed ZnO nanorods and nanoplates showed about 2 decades of linear
31 sensitivity range (0.1 mM – 9 mM) with good selectivity to ascorbic acid, dopamine, and fructose
32 [45]. Tarlani et. al. obtained different morphologies of nanostructured ZnO such as rod, powder,
33 particle, cube, rock candy-like, sheet, sphere, brain-like, groundnut-like and pussy willow-like by
34 utilizing aminoacids [46]. All these structures formulated by multi-walled carbon nanotubes on
35 glassy carbon electrode and were used to detect glucose. The best sensitivity was obtained from
36 the spherical ZnO nanostructures ($64.29 \mu\text{A mM}^{-1} \text{cm}^{-2}$) with a relatively short linear range (1 mM
37 – 10 mM). The selectivity against dopamine, uric acid and fructose were found to be satisfactory
38 and the sensors were stable over 30 days. Au nanostructures were functionalized using three-
39 dimensional hierarchical ZnO nano-architectures by Fang et. al. which resulted a short linear range
40 (1 mM – 20 mM) [47]. Selectivity was studied with good results against dopamine, uric acid and
41 fructose. The stability of sensors was tested for 15 days. Also, human serum samples were tested
42 with satisfactory results. ZnO hexagonal prisms with nickel nanostructures were used for non-
43
44
45
46
47
48
49
50
51
52
53
54
55
56
57
58
59
60

1
2
3 enzymatic glucose sensing by Yang et. al. with close to 3 decades of linear range (10 μM to 8.1mM)
4 [48]. Selectivity to distracter chemicals were good and the sensors were stable over 30 days. In
5 order to detect glucose levels from sweat, Munje et. al. developed a wearable, flexible
6 electrochemical glucose sensor based on sputtered ZnO electrodes [49]. Although the linear range
7 was not very wide, sensors were able to detect as low as 0.6 μM of glucose (sweat glucose levels
8 are much lower than blood glucose levels).
9

10
11
12
13
14 Titanium Oxide (TiO_2), a wide bandgap ($E_g = 3.2 \text{ eV}$) and intrinsically n-type semiconductor, has
15 been extensively investigated as a glucose biosensor. Luo et. al. investigated the glucose sensing
16 properties of highly dispersed titanium dioxide nanoclusters synthesized on reduced graphene
17 oxide [50]. Sensitivity levels of $35.8 \mu\text{A mM}^{-1} \text{ cm}^{-2}$ were observed. Selectivity experiments were
18 carried out with no apparent interference effects and the response time of the sensor was also
19 measured to be less than 10 seconds. Jang et. al. built a glucose biosensor based on the adsorption
20 of glucose oxidase at a TiO_2 -Graphene nanocomposite electrode with relatively low sensitivity (6.2
21 $\mu\text{A mM}^{-1} \text{ cm}^{-2}$) and a short linear range (1 mM – 8 mM) [51]. However, their synthesis of electrodes
22 (colloid dispersion) was simple and easy to repeat. A non-enzymatic glucose sensor was built by
23 depositing cobalt rich cobalt–copper alloy nanostructures on vertically aligned TiO_2 nanotube
24 arrays that resulted quite high sensitivity values ($4651.0 \mu\text{A mM}^{-1} \text{ cm}^{-2}$) [52]. The linear range was
25 up to 12 mM (lower limit was not mentioned in the article). A wide range of interferents and real
26 human serum were tested with good results.
27
28
29
30
31
32
33
34
35
36

37 Nickel Oxide (NiO), a p-type semiconductor, was also studied as a biosensing material. Liu et. al.
38 produced vertically aligned 3D porous NiO nanosheets on graphite disks by using chemical bath
39 deposition method [53]. This non-enzymatic glucose sensor had good anti-interference
40 performance against Uric Acid and Absorbic Acid and a fast response time ($<1 \text{ s}$). Linear range
41 was up to 10 mM with a moderate sensitivity value ($36.13 \mu\text{A mM}^{-1} \text{ cm}^{-2}$) and the sensors were
42 stable up to 14 days. Blood serum tests were also conducted with satisfactory results. Another non-
43 enzymatic NiO glucose sensor was produced by Prasad et. al. based on NiO nanostructures
44 decorated multi-walled carbon nanotubes [54]. Their sensor demonstrated moderate sensitivity
45 levels ($122.15 \mu\text{A mM}^{-1} \text{ cm}^{-2}$) up to 9 mM and higher sensitivity levels for lower concentration
46 ranges ($122.15 \mu\text{A mM}^{-1} \text{ cm}^{-2}$ for 1-200 μM). Sensors anti-interference and human serum response
47 were tested successfully. A relatively high sensitive ($1138 \mu\text{A mM}^{-1} \text{ cm}^{-2}$) NiO nanosheets were
48
49
50
51
52
53
54
55
56
57
58
59
60

1
2
3 prepared with graphene oxide films for non-enzymatic glucose sensing by Zhang et. al [55]. The
4 detection limit was found to be $0.18 \mu\text{M}$ but the linear range was too low ($1 \mu\text{M} - 0.4 \text{mM}$) to be
5 used for human glucose testing even though it showed good anti-interference and stability
6 performance. NiO thin films were magnetron sputtered on ITO substrates by Garcia et. al. that
7 exhibited high sensitivity ($1680 \mu\text{A mM}^{-1} \text{cm}^{-2}$), stability over 2 months, and anti-interference
8 performance against variety of interferents [56]. However, the linear range was relatively narrow
9 ($0 - 1.0 \text{mM}$) that limits the real-life application of this sensor.

10
11 Other metal oxides were also experimented for the glucose sensing applications. A conductometric
12 Tin Oxide (SnO_2) sensor with clinical linear range [57], an enzymatic, nanoporous Cerium oxide
13 (CeO_2) again with a clinical range and more than 6 weeks of shelf life [58], and Manganese Oxide
14 (Mn_xO_y) [59, 60] were experimented with some promise.

15
16 Table 1 shows representative glucose sensors with different metal oxide structure or types for
17 glucose sensors. Limit of detection, on the other hand, can be considered as the resolution.
18 Sensitivity values were also provided for comparison. Furthermore, in order to provide an insight
19 on the stability of each device, duration in days, relative standard deviation in percentage, and the
20 retention in percentage were also provided in Table 1.

21
22 In order to show the correlation between the linear range and the sensitivity with respect to different
23 metal oxides, Figure 1 was created by using the values from Table 1. Each vertical line represents
24 one particular article's performance in terms of linear range where the horizontal axis gives the
25 sensitivity value that was obtained for that particular sensor. It is obvious that CuO and ZnO have
26 higher sensitivity values with relatively wide linear range. TiO_2 sensors do not provide a wide
27 linear range and ZnO seems to have low sensitivity values. Although limited samples, SnO_2 and
28 Mn_xO_y did not show superior characteristics. However Cu_2O glucose sensor provided the best
29 sensitivity for the given wide linear range.

30
31 It is important to note here that the full functionality of a glucose sensor needs to be evaluated by
32 looking into anti-interference performance against lactose, fructose, mannose, ascorbic acid, uric
33 acid. Also, testing the device for real human blood serum gives the sensor a direct application
34 opportunities hence should be included in any research. Parameters such as stability and response
35 time are also important to measure. The authors believe that CuO and NiO are the most promising
36 metal oxides to be utilized in glucose sensing.

2.2. Urea and Uric Acid Sensors

Uric acid is a product of the metabolic breakdown of purines, which are found in cells and food products. Uric acid levels in blood are between 140 – 430 μM and abnormal uric acid values can lead to gout and kidney stones [61]. Traditionally, uric acid tests are conducted either via blood tests or through urine samples using color changing strips. There have been attempts to develop smaller scale uric acid sensing devices to lower the cost and applicability of uric acid measurements. Most designs focused on conductometric measurements using advanced materials to construct the electrodes in enzymatic or non-enzymatic sensors [62-64]. Urea, on the other hand, is a product of urea cycle occurring in human livers and kidneys where ammonia (NH_3) is dissolved into urea ($(\text{NH}_2)_2\text{CO}$) [65]. Urea is considered a waste product and excreted via urine and sweat. Urea levels are within 2.5 – 7.5 mM in blood and abnormal urea levels can lead to kidney and liver problems such as renal failures and uremia (excessive urea in blood) [66].

Urea sensors: Vertically aligned ZnO nanorods were used as urea sensors within the linear range of 0.001–24.0 mM but relatively low sensitivity ($41.64 \mu\text{A mM}^{-1} \text{cm}^{-2}$) [67]. However, sensors showed good anti-interference capability and stability. Highest sensitivity value for urea sensors was achieved by Tak et. al. by exploiting the large surface to volume ratio of flower-like ZnO nanostructures in a range of 1.65 mM to 16.50 mM [68]. Sensitivity value was determined to be $132 \mu\text{A mM}^{-1} \text{cm}^{-2}$ with a tested response time of 4 s. However, cross-sensitivity and durability tests were not performed. An electrochemically deposited nanostructured ZnO films showed similar linear range (1.7 - 13.6 mM) but a smaller sensitivity values ($40 \mu\text{A/mM}^{-1}\text{cm}^{-2}$) [69].

Besides ZnO, some other NMOs were also experimented towards urea sensing such as non-enzymatic SnO₂ thin films [70], very stable (6 months) but less sensitive ($3.7 \mu\text{A mM}^{-1} \text{cm}^{-2}$) enzymatic CeO₂ thin films [71], enzymatic NiO nanostructures thin films with low sensitivity ($21.3 \mu\text{A mM}^{-1} \text{cm}^{-2}$) [72], and non-enzymatic Ni/CoO films with relatively good sensitivity of $166 \mu\text{A mM}^{-1}\text{cm}^{-2}$ but for a limited linear range (0.06 mM – 0.30 mM) [73].

Uric acid sensors: 3D periodic mesoporous nickel oxide (NiO) particles with crystalline walls and a moderate sensitivity ($756.26 \mu\text{A mM}^{-1} \text{cm}^{-2}$) levels were achieved for uric acid detection up to 0.374 mM [74]. However, this work did not conduct and interference studies. NiO thin films were used on platinum coated glass substrates to uric acid levels with a relatively high sensitivity ($1278.48 \mu\text{A/mM}$) that covered the clinical human uric acid levels (0.05 mM - 1.0mM) [75]. Same

group worked on growing CuO thin films on platinum coated glass substrates for uric acid measurements with a relatively high sensitivity $2700 \mu\text{A mM}^{-1}\text{cm}^{-2}$ [76]. The sensor was stable for more than 14 weeks and selective to glucose, cholesterol, urea, ascorbic acid, and lactic acid.

Table 2 summarizes the specifications of some urea sensors based on metal oxide structures. Similar to Table 1, limit of detection, detection range, sensitivity and K_{mapp} values were provided along with the specific metal oxide structures and stability parameters. Here, it must be noted that some values were converted from mg/dL to mM by using the molar mass of urea (60.056 g/mol).

Figure 2 shows the overall summary of each sensor's linear range and sensitivity. It can clearly be seen that uric acid sensors tend to have a higher sensitivity. Although the linear range seems limited, the devices are suitable for the clinical blood uric acid levels. Also, CuO and NiO films provide a better sensitivity. It must be noted here that all uric acid sensors based on NMOs were thin films. Urea sensors, on the other hand, are mostly achieved through enzymatic reactions and with low sensitivity values. Linear ranges are about the same for each sensor but a composite NiO/CoO film provided significantly higher sensitivity.

2.3. Cholesterol Sensors

Cholesterol is an organic molecule that is synthesized by the human body to maintain the cell membrane temperature. High levels of cholesterol can narrow the arteries and increase the risk of heart disease. ZnO was one of the most used materials for cholesterol sensing. ZnO nanorods on Silver electrodes for cholesterol sensing reached a sensitivity of $74.10 \mu\text{A mM}^{-1}\text{cm}^{-2}$ at a detection limit of $0.0015 \mu\text{M}$ [77]. Response time was less than 2 s and nanorods were stable for over 45 days. Flower-shaped ZnO nanorods were also fabricated with a sensitivity of $61.7 \mu\text{A}\mu\text{M}^{-1}\text{cm}^{-2}$ at a response time less than 5 s [78]. However, this structure was tested for only very low levels of cholesterol (1.0–15.0 μM), which would not make it suitable for human serum samples [78]. ZnO nanotube arrays on Si/Ag substrate were fabricated enzymatic cholesterol sensors [79]. The sensitivity value was $79.40 \mu\text{A}\mu\text{M}^{-1}\text{cm}^{-2}$ and a linear range of 1.0 μM - 13.0 mM. A fast response time (~2 s) and a low detection limit (0.5 nM) were reported and the sensors were tested with human blood serum [79]. A solution-gated, enzymatic, field-effect-transistor by using vertically aligned ZnO nanorods were realized with reported selectivity to electroactive agents [80]. Linear

range was 0.001–45mM with a moderate sensitivity ($10 \mu\text{A mM}^{-1} \text{cm}^{-2}$), and a detection limit (0.05 mM) were obtained [80]. Wang et al aimed to use a novel method for the fabrication of gold/platinum hybrid functionalized ZnO nanorods and multi-walled carbon nanotubes. They achieved a moderate linear range (0.1 μM - 759.3 μM), a low detection limit (0.03 μM), but a low sensitivity ($26.8 \mu\text{A mM}^{-1} \text{cm}^{-2}$) values [81]. One alternative to increase the sensitivity of ZnO based cholesterol sensors is to create composite matrixes. One good candidate is CuO, which offers higher sensitivity with a drawback of lower stability values. A ZnO–CuO composite matrix on to indium tin oxide substrates via pulsed laser deposition resulted in a sensitivity of $760 \mu\text{A mM}^{-1} \text{cm}^{-2}$ and a 5 s response time [82]. The concentration range of the composite matrix fell between 0.5 mM to 12mM.

Different metal oxides were experimented in order to reach high sensitivity values. Ansari et al deposited a chitosan-tin oxide (SnO_2) nanobiocomposite film onto ITO substrates for enzymatic cholesterol detection that resulted in a high sensitivity value ($1300 \mu\text{A mM}^{-1} \text{cm}^{-2}$) [83]. The sensor retained 95% of its enzyme activity after 4 – 6 weeks. Chitosan was also used in CeO_2 NMOs to increase the stability. The physiosorption technique was utilized to obtain a linear detection range of 0.2 – 10.4 mM with a sensitivity of $1807 \mu\text{A mM}^{-1} \text{cm}^{-2}$ for Chitosan stabilized CeO_2 films, which were stable over 60 days and exhibited good selectivity [84]. Another CeO_2 films were fabricated using sol-gel method with a very high sensitivity ($80000 \mu\text{A mM}^{-1} \text{cm}^{-2}$) with a wide linear detection range (0.2 – 10.4 mM) [85]. NiO and MnO_2 were also experimented to develop cholesterol sensors but the sensitivity values were quite low [86, 87].

Table 3 summarizes the limited literature on nanostructured metal oxide based cholesterol sensors in a similar fashion of Table 1 and 2. Similar to some urea sensors, some cholesterol sensors' units were converted from mg/dL to mM by using the molar mass of the cholesterol (386.65 g/mol). It can be seen from Table 3 that ZnO was the most experimented metal oxides. It is promising to create composite structures with CuO and ZnO to increase the sensitivity values. Although very high sensitivity values were obtained for CeO_2 , it must be noted here that these sensors are rely on enzymatic reactions and would be affected by environmental conditions such as pH and temperature. Figure 3 also shows the summary of the sensitivity values for cholesterol sensors.

2.4. Other Sensor Applications

1
2
3 Although glucose, uric acid, and cholesterol are the most investigated biological sensors using
4 metal oxide nanostructures as a platform, there were several other metal oxide-based sensing
5 systems worth mentioning in this review article.
6
7

8
9 Hydrogen peroxide (H_2O_2) sensing is another popular application of metal oxide nanostructures.
10 Copper(II) oxide nanorod bundles modified by basal plane pyrolytic graphite electrode were
11 developed by McAuley et al [88]. The limit of detection and sensitivity values were measured to
12 be $0.2 \mu M$ with a sensitivity of $0.15 \mu A/\mu M$ [88]. Multi walled carbon nanotubes were combined
13 with CuO nanoflower-modified electrodes by Zhang et al for H_2O_2 detection with detection range
14 of $0.5 - 82 \text{ mM}$ and sensitivity value $0.16 \mu M$ [89]. Gu et al produced gold electrodes modified
15 three-dimensional (3D) CuO flower-like nanostructures for H_2O_2 sensing with a detection range of
16 $50 - 750 \mu M$ and a sensitivity of $116.1 \mu A/mM$ [90]. ZnO micro-pompons were simultaneously
17 deposited with gold electrodes by Zhou et. al. with a linear range of $0.2 - 3.4 \text{ mM}$, sensitivity of
18 $1395.64 \mu A/mM^{-1}cm^{-2}$, and a response time of less than 4 s [91]. Chirizziet et.al. proposed an
19 approach based on the immobilization of cupric/cuprous oxide core shell nanowires that resulted a
20 sensitivity of $2.793 \mu A/mM$ with a detection limit of $0.35 \mu M$ [92]. Porous Cerium dioxide
21 nanostructured films were also used by Yagati et al as H_2O_2 sensing with a limit of detection 0.6
22 μM and linearity up to $3mM$ [93]. The response time of the sensor was measured to be 8 s with a
23 sensitivity of $5.4 \mu A/mM^{-1}cm^{-2}$ [193]. Gold nanoparticles aggregates were assembled with
24 manganese dioxide (MnO_2) nanoparticles by Li et al for a hydrogen peroxide sensing range of 0.78
25 μM to $836 \mu M$ with a sensitivity of $53.5 \mu A/cm^2$ and a detection limit of 46.8 nM [94]. Bracamonte
26 et. al. used CeO_2 to detect H_2O_2 . The sensitivity range was obtained as $160 \mu A \text{ cm}^{-2} \text{ mM}^{-1}$ [95].
27
28
29
30
31
32
33
34
35
36
37
38
39

40 Sequence-specific target DNA detection was explored by Yuzhong et al by introducing gold
41 nanoparticles onto the surface of CuO nanospindles deposited onto glassy carbon electrodes [96].
42 With a good selectivity, proposed DNA biosensor has a linear concentration range of 0.1 pM to 1
43 μM with a detection limit of 35 fM which could distinguish a single-mismatched target DNA [96].
44 Another DNA sensor was realized by using nanostructured zirconium oxide with Escherichia coli
45 (*E. coli*) single stranded DNA with a detection range of 10^{-6} to 10^6 pM [97]. Another DNA type
46 biosensor was developed for detection of bacterial meningitis by using flower-like ZnO
47 nanostructures Pt/Si substrates, which exhibited a sensitivity of $168.64 \mu A/ng/\mu l/cm^2$ with a
48 detection limit of about $5ng/\mu l$ [98].
49
50
51
52
53
54
55
56
57
58
59
60

1
2
3 Vibrio cholera detection was employed by using nanostructured magnesium oxide films on ITO
4 glass substrates [99]. Patel et al reported a cholera detection sensitivity of 16.80 nA/ng/cm^2 , fast
5 response time (less than 3s), and linearity between 100 to 500 ng/L that is stable for 120 days [99].
6
7 CuO nanoparticles were also explored for sweat electrolyte sensing via resistive measurement
8 techniques by Sahin et al using artificial sweat as the analyte [100, 101]. Their work centered
9 around sodium and potassium doping and annealing effects of CuO fabrication [101].
10
11 Roychoudhury et al developed a dopamine biosensor using nickel oxide nanoparticles
12 demonstrating a sensitivity of $0.06 \text{ }\mu\text{A}/\mu\text{M}$ in a linear range of $2 \text{ }\mu\text{M}$ to $100 \text{ }\mu\text{M}$ with a detection
13 limit of $1.04 \text{ }\mu\text{M}$ [102]. The sensor had a response time of 45 s with long shelf life of 45 days [102].
14
15 Azzouzi et al produced an amperometric biosensor based on graphene oxide for the detection of L-
16 lactate tumor biomarker with a linear detection of $10 \text{ }\mu\text{M}$ – 5 mM , sensitivity of $154 \text{ }\mu\text{A/mM/cm}^2$,
17 and a detection limit of $0.13 \text{ }\mu\text{M}$. [103].
18
19
20
21
22
23
24
25
26
27
28

29 **3. Conclusion and future perspectives**

30
31 In this review, we focused on most common sensing analytes such as glucose, urea and uric acid,
32 and cholesterol by organizing each section with different types of NMOs. Corresponding tables for
33 each section summarized the sensing parameters of the devices. Sensitivity, limit of detection,
34 detection range, K_{mapp} value, stability duration, relative standard deviation, and retention, and the
35 sensing type were provided for each article where available. Some other applications of NMOs
36 such as hydrogen peroxide and DNA sensing were provided as well as some unconventional
37 sensing approaches. Representative figures from literature were used to give a visual illustration of
38 the data and nanostructures.
39
40
41
42
43
44

45 It can be seen from our extensive literature review that there is a wide variety of techniques utilized
46 to incorporate NMOs in electrochemical biosensors. Those who are interested in working on NMOs
47 should first decide on the technique to move forward. Like any biosensors, sensitivity, selectivity,
48 response time, and stability are main characteristics to determine if the proposed approach is
49 valuable. Although new advances in technology allow more sophisticated manufacturing methods,
50 there is still some “art” in producing consistent films. One should be looking into more robust,
51 repeatable manufacturing schemes. Biosensors are ultimately to be used in clinical applications.
52
53
54
55
56
57
58
59
60

1
2
3 Currently, NMOs have yet to be explored fully for their capabilities in real-life scenarios with
4 application-specific issues such as durability, energy efficiency, and environmental conditions.
5 Manufacturing NMO based biosensors should also be explored in terms of accuracy, calibration
6 techniques, and robustness. Also, sample matrices that electrodes are applied to are very important
7 and directly affects the sensing properties. Therefore, a detailed study should be carried out to
8 investigate the effects of fabrication methodologies. It is also known that every time a film is used
9 for sensing, the surface chemistry is altered. Therefore, a careful study of the sensors should be
10 done by looking into the isoelectric point (IEP) of the surface to make sure the surface still stays
11 active.
12
13
14
15
16
17
18

19 **Acknowledgements**

20
21 Authors thank Thomas White and Andrew Brueck for their careful proof-reading and Drs Anja
22 Mueller, Thompson Mefford, and Ben Alper for fruitful discussions.
23
24

25 **References**

- 26
27
28 [1] A.Tereshchenko, M. Bechelany, R. Viter, V. Khranovskyy, V. Smyntyna, N. Starodub,
29 R.Yakimova, Optical Biosensors Based on ZnO Nanostructures: Advantages and Perspectives. A
30 Review, Sensors and Actuators B (dx.doi.org/doi:10.1016/j.snb.2016.01.099)
31
32
33 [2] S. K. Arya, S. Saha, J. E. Ramirez-Vick, V. Gupta, S. Bhansali, S. P. Singh, Recent advances
34 in ZnO nanostructures and thin films for biosensor applications: Review, Analytica Chimica Acta
35 737 (2012) 1– 21.
36
37
38 [3] J. Li, Y. Duan, H. Hu, Y. Zhao, Q. Wang, Flexible NWs sensors in polymer, metal oxide and
39 semiconductor materials for chemical and biological detection, Sensors and Actuators B 219
40 (2015) 65–82.
41
42
43 [4] S Shi, L. Wang, R. Su, B. Liu, R. Huang, W. Qi, Z. He, A polydopamine-modified optical fiber
44 SPR biosensor using electroless-plated gold films for immunoassays, Biosensors and
45 Bioelectronics 74 (2015) 454–460.
46
47
48 [5] X. Jia, S. Dong, E. Wang, Engineering the bioelectrochemical interface using functional
49 nanomaterials and microchip technique toward sensitive and portable electrochemical biosensors,
50 Biosensors and Bioelectronics 76 (2016) 80–90.
51
52
53
54
55
56
57
58
59
60

- [6] M. Jacobs, S. Muthukumar, A. P.Selvam, J. E. Craven , S. Prasad, Ultra-sensitive electrical immunoassay biosensors using nanotextured zinc oxide thin films on printed circuit board platforms, *Biosensors and Bioelectronics* 55 (2014) 7–13.
- [7] J. Chao, D. Zhu, Y.Zhang, L. Wang, C. Fan, DNA nanotechnology-enabled biosensors, *Biosensors and Bioelectronics* 76 (2016) 68–79.
- [8] H. Li, Y. Guo, L. Xiao, B. Chen, A fluorometric biosensor based on H₂O₂-sensitive nanoclusters for the detection of acetylcholine, *Biosensors and Bioelectronics* 59 (2014) 289–292.
- [9] Guo-Jun Zhang, Yong Ning, Silicon nanowire biosensor and its applications in disease diagnostics:A review, *Analytica Chimica Acta* 749 (2012) 1– 15.
- [10] Y. Song, Y. Luo, C. Zhu, H. Li , D. Du, Y. Lin, Recent advances in electrochemical biosensors based on graphene two-dimensional nanomaterials, *Biosensors and Bioelectronics* 76 (2016) 195–212.
- [11] Y. Cui, Q.Q. Wei, H.K. Park, C.M. Lieber, Nanowire nanosensors for highly sensitive and selective detection of biological and chemical species. *Science* 293 (2001) 1289–1292.
- [12] Ahmad Umar M.M. Rahman, A. Al-Hajry, Y.-B. Hahn, Highly-sensitive cholesterol biosensor based on well-crystallized flower-shaped ZnO nanostructures, *Talanta* 78 (2009) 284–289.
- [13] G. Korotcenkov, S.D. Han, B.K. Cho, V. Brinzari, Grain size effects in sensor response of nanostructured SnO₂- and In₂O₃-based conductometric gas sensor, *Crit. Rev. Solid State Mater. Sci.* 34 (1–2) (2009) 1–17.
- [14] R.L. Vander Wal, G.W. Hunter, J.C. Xub, M.J. Kulis, G.M. Berger, T.M. Tich, Metal-oxide nanostructure and gas-sensing performance, *Sensors and Actuators B* 138 (2009) 113–119.
- [15] C.N. Xu, J. Tamaki, N. Miura, N. Yamazoe, Grain size effects on gas sensitivity of porous SnO₂-based elements, *Sens. Actuators B* 3 (1991) 147–155.
- [16] B. Sahin, T. Kaya. “Enhanced hydration detection properties of nanostructured CuO films by annealing ”. *Microelectronical Engineering* 164 (2016) 88–92.
- [17] V.Manthina, A. G. Agrios, Single-pot ZnO nanostructure synthesis by chemical bath deposition and their applications, *Nano-Structures & Nano-Objects* 7 (2016) 1–11.

- [18] A. Nebatti, C. Pflitsc , B. Atakan, Unusual application of aluminium-doped ZnO thin film developed by metalorganic chemical vapour deposition for surface temperature sensor, *Thin Solid Films* 636 (2017) 532–536.
- [19] M. Taheri, H. Abdizadeh , M. R. Golobostanfard, Formation of urchin-like ZnO nanostructures by sol-gel electrophoretic deposition for photocatalytic application, *Journal of Alloys and Compounds* 725 (2017) 291-301.
- [20] Z.E. Vakulov, E.G. Zamburg, D.A. Khakhulin, O.A. Ageev, Thermal stability of ZnO thin films fabricated by pulsed laser deposition, *Materials Science in Semiconductor Processing* 66 (2017) 21–25.
- [21] Y.Hahn, R. Ahmadw, N. Tripathyw, Chemical and biological sensors based on metal oxide nanostructures, *Chem. Commun.*, 48,(2012) 10369–10385.
- [22] M. M. Rahman, A. J. S.Ahammad , J.Jin , S. J. Ahn and J. Lee, A Comprehensive Review of Glucose Biosensors Based on Nanostructured Metal-Oxides, *Sensors* 10 (2010) 4855-4886.
- [23] A. Liu, Towards Development of Chemosensors and Biosensors with Metal-Oxide-Based Nanowires or Nanotubes. *Biosens. Bioelectron.* 24 (2008) 167–177.
- [24] C.L. Hsu, J. Y. Tsai , T. J. Hsueh, Ethanol gas and humidity sensors of CuO/Cu₂O composite nanowires based on a Cu through-silicon via approach, *Sensors and Actuators B* 224 (2016) 95–102.
- [25] S. J. Patil, A. V. Patil, C. G. Dighavkar, K. S. Thakare, R. Y. Borase, S. J. Nandre, N.G.Deshpande, R. R. Ahire, Semiconductor metal oxide compounds based gas sensors: A literature review, *Front. Mater. Sci.* 2015, 9(1): 14–37.
- [26] S. Mallakpour, M. Madani, A review of current coupling agents for modification of metal oxide nanoparticles, *Progress in Organic Coatings* 86 (2015) 194–207.
- [27] N. S. Oliver, C. Toumazou, A. E. G. Cass, D. G. Johnston, Glucose sensors: a review of current and emerging technology, *Diabetic Medicine*, 26(3) (2009) 197-210.
- [28] H. C. Wang, A. R. Lee, Recent developments in blood glucose sensors. *Journal of Food and Drug Analysis.* 23 (2015) 191-200.
- [29] F. Cao, J. Gong, Nonenzymatic glucose sensor based on CuO microfibers composed of CuO nanoparticles. *Analytica chimica acta*, 723 (2012) 39-44.

- [30] J. X. Wang, X. W. Sun, A. Wei, Y. Lei, X. P. Cai, C. M. Li, Z. L. Dong, Zinc oxide nanocom biosensor for glucose detection, *Applied Physics Letters* 88 (2006) 233106.
- [31] H. N. Choi, M. A. Kim, W. Y. Lee, Amperometric glucose biosensor based on sol-gel-derived metal oxide/Nafion composite films, *Analytica Chimica Acta* 537 (2005) 179–187.
- [32] X. Wanga, C. Hua, H. Liub, G. Dub, X. Hea, Y. Xi, Synthesis of CuO nanostructures and their application for nonenzymatic glucose sensing, *Sensors and Actuators B* 144 (2010) 220–225.
- [33] S. Saha, S. K. Arya, S.P. Singh, K. Sreenivas, B.D. Malhotra, V. Gupta, Nanoporous cerium oxide thin film for glucose biosensor, *Biosensors and Bioelectronics* 24 (2009) 2040–2045.
- [34] H. Liu, X. Wu, B. Yang, Z. Li, L. Lei, X. Zhang, Three-Dimensional Porous NiO Nanosheets Vertically Grown on Graphite Disks for Enhanced Performance Non-enzymatic Glucose Sensor, *Electrochimica Acta* 174 (2015) 745–752.
- [35] S. H. Lee, J. Yang, Y. J. Han, M. Cho, Y. Lee, Rapid and highly sensitive MnOxnanorods array platform for aglucose analysis, *Sensors and Actuators B* 218 (2015) 137–144.
- [36] X. Zhang, G. Wang, X. Liu, J. Wu, M. Li, J. Gu, H. Liu, B. Fang, Different CuO Nanostructures: Synthesis, Characterization, and Applications for Glucose Sensors, *J. Phys. Chem. C* 112 (2008) 16845–16849.
- [37] G Filipic, U Cvelbar, Copper oxide nanowires: a review of growth, *Nanotechnology* 23 (2012) 194001 (16pp).
- [38] K. Li, Guoli Fan, Lan Yang, Feng Li, Novel ultrasensitive non-enzymatic glucose sensors based oncontrolled flower-like CuO hierarchical films, *Sensors and Actuators B* 199 (2014) 175–182.
- [39] X. Zhang, G. Wang, X. Liu, J. Wu, M. Li, J. Gu, H. Liu, B. Fang, Different CuO Nanostructures: Synthesis, Characterization, and Applications for Glucose Sensors, *J. Phys. Chem. C* 112 (2008) 16845–16849.
- [40] Y. Li, Y. Wei, G. Shi, Y. Xian, L. Jin, Facile Synthesis of Leaf-Like CuO Nanoparticles and Their Application on Glucose Biosensor, *Electroanalysis* , 23, (2011) 497 – 502.
- [41] X. Wang, C. Hu, H. Liu, G. Du, X. He, Y. Xi, Synthesis of CuO nanostructures and their application for nonenzymatic glucose sensing, *Sensors and Actuators B* 144 (2010) 220–225.

- [42] S. H. Kim, A. Umar, S. W. Hwang, Rose-like CuO nanostructures for highly sensitive glucose chemical sensor application, *Ceramics International* 41(2015) 9468–9475.
- [43] R. Khan, R. Ahmad, P. Rai, L. W. Jang, J. H. Yun, Y. T. Yu, Y. B. Hahn, I. H. Lee, Glucose-assisted synthesis of Cu₂O shuriken-like nanostructures and their application as nonenzymatic glucose biosensors, *Sensors and Actuators B* 203 (2014) 471–476.
- [44] J. X. Wang, X. W. Sun, A. Wei, Y. Lei, X. P. Cai, C. M. Li, Z. L. Dong, Zinc oxide nanocomb biosensor for glucose detection, *Applied Physics Letters* 88, (2006) 233106.
- [45] Y. Zhai, Shengyong Zhai, G. Chen, K. Zhang, Q. Yue, L. Wang, J. Liu, J. Jia, Effects of morphology of nanostructured ZnO on direct electrochemistry and biosensing properties of glucose oxidase, *Journal of Electroanalytical Chemistry* 656 (2011) 198–205.
- [46] A. Tarlani, M. Fallah, B. Lotfi, A. Khazraei, S. Golsanamlou, J. Muzart, M. M. Aghayan, New ZnO nanostructures as non-enzymatic glucose biosensors, *Biosensors and Bioelectronics* 67 (2015) 601–607.
- [47] L. Fang, B. Liu, L. Liua, Y. Lia, K. Huang, Q. Zhang, Direct electrochemistry of glucose oxidase immobilized on Au nanoparticles-functionalized 3D hierarchically ZnO nanostructures and its application to bioelectrochemical glucose sensor, *Sensors and Actuators B* 222 (2016) 1096–1102.
- [48] Y. Yang, Y. Wang, X. Bao, H. Li, Electrochemical deposition of Ni nanoparticles decorated ZnO hexagonal prisms as an effective platform for non-enzymatic detection of glucose, *Journal of Electroanalytical Chemistry* 775 (2016) 163–170.
- [49] R. D. Munje, S. Muthukumar, S. Prasad, Lancet-free and label-free diagnostics of glucose in sweat using ZincOxide based flexible bioelectronics, *Sensors and Actuators B* 238 (2017) 482–490.
- [50] Z. Luo, X. Ma, D. Yang, L. Yuwen, X. Zhu, L. Weng, L. Wang, Synthesis of highly dispersed titanium dioxide nanoclusters on reduced graphene oxide for increased glucose sensing, *Carbon* 57 (2013) 470–476.
- [51] H. D. Jang, S. K. Kim, H. Chang, K. M. Roh, J. W. Choi, J. Huang, A glucose biosensor based on TiO₂–Graphene composite, *Biosensors and Bioelectronics* 38 (2012) 184–188.

- [52] P.V. Suneesh, V. S. Vargis, T. Ramachandran, B. G. Nair, T.G. S. Babu, Co–Cu alloy nanoparticles decorated TiO₂ nanotube arrays for highly sensitive and selective nonenzymatic sensing of glucose, *Sensors and Actuators B* 215 (2015) 337–344.
- [53] H. Liu, X. Wu, B. Yang, Z. Li, L. Lei, X. Zhang, Three-Dimensional Porous NiO Nanosheets Vertically Grown on Graphite Disks for Enhanced Performance Non-enzymatic Glucose Sensor, *Electrochimica Acta* 174 (2015) 745–752.
- [54] R. Prasad, B. R. Bhat, Multi-wall carbon nanotube–NiO nanoparticle composite as enzyme-free electrochemical glucose sensor, *Sensors and Actuators B* 220 (2015) 81–90.
- [55] H. Zhang, S. Liu, Nanoparticles-assembled NiO nanosheets templated by grapheneoxide film for highly sensitive non-enzymatic glucose sensing, *Sensors and Actuators B* 238 (2017) 788–794.
- [56] F.J. Garcia-Garcia, P. Salazar, F. Yubero, A.R. González-Elipé, Non-enzymatic Glucose electrochemical sensor made of porous NiO thin films prepared by reactive magnetron sputtering at oblique angles, *Electrochimica Acta* 201 (2016) 38–44.
- [57] K. S. Mahadeva, J. Kim, Conductometric glucose biosensor made with cellulose and tin oxide hybrid nanocomposite, *Sensors and Actuators B* 157 (2011) 177– 182.
- [58] S. Saha, S. K. Arya, S.P. Singh, K. Sreenivas, B.D. Malhotra, V. Gupta, Nanoporous cerium oxide thin film for glucose biosensor, *Biosensors and Bioelectronics* 24 (2009) 2040–2045.
- [59] S. H. Lee, J. Yang, Y. J. Han, M. Cho, Y. Lee, Rapid and highly sensitive MnO_x nanorods array platform for a glucose analysis, *Sensors and Actuators B* 218 (2015) 137–144.
- [60] S. Yang, L. Liu, G. Wang, G. Li, D. Deng, L. Qu, One-pot synthesis of Mn₃O₄ nanoparticles decorated with nitrogen-doped reduced graphene oxide for sensitive nonenzymatic glucose sensing, *Journal of Electroanalytical Chemistry* 755 (2015) 15–21.
- [61] X. Chen, G. Wu, Z. Cai, M. Oyama, X. Chen, Advances in enzyme-free electrochemical sensors for hydrogen peroxide, glucose, and uric acid. *Microchimica Acta*, 181 (2014) 689-705.
- [62] M. M. Castillo-Ortega, D. E. Rodriguez, J. C. Encinas, M. Plascencia, F. A. Mendez-Velarde, R. Olayo, Conductometric uric acid and urea biosensor prepared from electroconductive polyaniline–poly (n-butyl methacrylate) composites. *Sensors and Actuators B: Chemical*, 85(1) (2002) 19-25.

- [63] S.G. Ansari, R. Wahab, Z.A. Ansari, Y. S. Kima, G. Khang, A. Al-Hajryd, H.S. Shin, Effect of nanostructure on the urea sensing properties of sol-gel synthesized ZnO, *Sensors and Actuators B* 137 (2009) 566–573
- [64] J. C. Chen, H. H. Chung, C. T., Hsu, D. M. Tsai, A. S. Kumar, J. M. Zen, A disposable single-use electrochemical sensor for the detection of uric acid in human whole blood. *Sensors and Actuators B: Chemical*, 110(2) (2005) 364-369.
- [65] N. S. Nguyen, G. Das, H. H. Yoon, Nickel/cobalt oxide-decorated 3D graphene nanocomposite electrode for enhanced electrochemical detection of urea, *Biosensors and Bioelectronics* 77 (2016) 372–377
- [66] Z. Yang, X. Liu , C. Zhang, B. Liu, A high-performance nonenzymatic piezoelectric sensor based on molecularly imprinted transparent TiO₂ film for detection of urea, *Biosensors and Bioelectronics* 74 (2015) 85–90.
- [67] R. Ahmad, N. Tripathy, Y. B. Hahn, Highly stable urea sensor based on ZnO nanorods directly grown on Ag/glass electrodes, *Sensors and Actuators B* 194 (2014) 290– 295.
- [68] M. Tak, V. Gupta, M. Tomar, A highly efficient urea detection using flower-like zinc oxide nanostructures, *Materials Science and Engineering C* 57 (2015) 38–48.
- [69] A.Ali, A. A. Ansari, A. Kaushik, P. R. Solanki, A. Barik, M.K. Pandey, B.D. Malhotra, Nanostructured zinc oxide film for urea sensor, *Materials Letters* 63 (2009) 2473–2475.
- [70] S.G. Ansari, H. Fouad, H.S. Shin, Z.A. Ansari, Electrochemical enzyme-less urea sensor based on nano-tin oxide synthesized by hydrothermal technique, *Chemico-Biological Interactions* 242 (2015) 45-49.
- [71] A. A. Ansari, M. Azahar, B. D. Malhotra, Electrochemical Urea Biosensor Based on Sol-gel Derived Nanostructured Cerium Oxide, *Journal of Physics: Conference Series* 358 (2012) 012006.
- [72] M. Tyagi, M. Tomar, V. Gupta, NiO nanoparticle-based urea biosensor, *Biosensors and Bioelectronics* 41 (2013) 110–115.
- [73] N. Si Nguyen, G. Das, H. H. Yoon, Nickel/cobalt oxide-decorated 3D graphene nanocomposite electrode for enhanced electrochemical detection of urea, *Biosensors and Bioelectronics* 77 (2016) 372–377.
- [74] W. Huang, Y. Cao, Y.Chen, Y. Zhou, . Q. Huang, 3-D Periodic Mesoporous Nickel Oxide for Nonenzymatic Uric Acid Sensors With Improved Sensitivity, *Applied Surface Science* 359 (2015) 221–226.

- [75] K.Arora, M. Tomar, V. Gupta, Highly sensitive and selective uric acid biosensor based on RF sputtered NiO thin film, *Biosensors and Bioelectronics* 30 (2011) 333–336.
- [76] K. Jindal, M. Tomar, V. Gupta, CuO thin film based uric acid biosensor with enhanced response characteristics, *Biosensors and Bioelectronics* 38 (2012) 11–18.
- [77] R. Ahmad, N. Tripathy, Y.B. Hahn, Wide linear-range detecting high sensitivity cholesterol biosensors based on aspect-ratio controlled ZnO nanorods grown on silver electrodes, *Sensors and Actuators B* 169 (2012) 382– 386.
- [78] A. Umar, M.M. Rahman, A. Al-Hajry, Y.B. Hahn, Highly-sensitive cholesterol biosensor based on well-crystallized flower-shaped ZnO nanostructures, *Talanta* 78 (2009) 284–289.
- [79] R. Ahmad, N. Tripathy, S. H. Kim, A. Umar, A. Al-Hajry, Y. B. Hahn, High performance cholesterol sensor based on ZnO nanotubes grown on Si/Ag electrodes, *Electrochemistry Communications* 38 (2014) 4–7.
- [80] R. Ahmad, N. Tripathy , Y. B. Hahn, High-performance cholesterol sensor based on the solution-gated field effect transistor fabricated with ZnO nanorods, *Biosensors and Bioelectronics* 45 (2013) 281–286.
- [81] C. Wang, X. Tan, S. Chen, R.Yuan, F. Hu, D. Yuan, Y. Xiang, Highly-sensitive cholesterol biosensor based on platinum–gold hybrid functionalized ZnO nanorods, *Talanta* 94 (2012) 263–270.
- [82] N. Batra, M. Tomar, V. Gupta, ZnO–CuO composite matrix based reagentless biosensor for detection of total cholesterol, *Biosensors and Bioelectronics* 67(2015) 263–271.
- [83] A. A. Ansari, A. Kaushik, P. R. Solanki, B. D. Malhotra, Electrochemical Cholesterol Sensor Based on Tin Oxide-Chitosan Nanobiocomposite Film, *Electroanalysis* 21, (2009) 965 – 972.
- [84] B. D. Malhotra, A. Kaushik, Metal oxide–chitosan based nanocomposite for cholesterol biosensor, *Thin Solid Films* 518 (2009) 614–620.
- [85] A. A. Ansari, A. Kaushik, P.R. Solanki, B.D. Malhotra, Sol–gel derived nanoporous cerium oxide film for application to cholesterol biosensor, *Electrochemistry Communications* 10 (2008) 1246–1249.
- [86] J. Singh, P. Kalita, M. K. Singh, B. D. Malhotra, Nanostructured nickel oxide-chitosan film for application to cholesterol sensor, *Applied Physics Letters* 98 (2011) 123702-123706.
- [87] C. Charan, V. K. Shahi, Nanostructured manganese oxide–chitosan-based cholesterol Sensor, *J Appl Electrochem* 44 (2014) 953–962

[88] C. Batchelor-McAuleya, Y. Dub, G. G. Wildgoose, R. G. Compton, The use of copper(II) oxide nanorod bundles for the non-enzymatic voltammetric sensing of carbohydrates and hydrogen peroxide, *Sensors and Actuators B* 135 (2008) 230–235.

[89] K. Zhang, N. Zhang, H. Cai, C. Wang, A novel non-enzyme hydrogen peroxide sensor based on an electrode modified with carbon nanotube-wired CuO nanoflowers, *Microchim Acta* 176 (2012) 137–142.

[90] A. Gu, G. Wang, X. Zhang, B. Fang, Synthesis of CuO nanoflower and its application as a H₂O₂ sensor, *Bull. Mater. Sci.*, 33 (2010) 17–20.

[91] Y. Zhou, L. Wang, Z. Ye, M. Zhao, J. Huang, Synthesis of ZnO micro-pompons by soft template-directed wet chemical method and their application in electrochemical biosensors, *Electrochimica Acta* 115 (2014) 277–282.

[92] D. Chirizzi, M. R. Guascito, E. Filippo, C. Malitesta, A. Tepore, A novel nonenzymatic amperometric hydrogen peroxide sensor based on CuO@Cu₂O nanowires embedded in to poly (vinylalcohol), *Talanta* 147 (2016) 124–131.

[93] A. K. Yagati, T. Lee, J. Min, J. W. Choi, An enzymatic biosensor for hydrogen peroxide based on CeO₂ nanostructure electrodeposited on ITO surface, *Biosensors and Bioelectronics* 47(2013) 385–390.

[94] Y. Li, J. Zhang, H. Zhu, F. Yang, X. Yang, Gold nanoparticles mediate the assembly of manganese dioxide nanoparticles for H₂O₂ amperometric sensing, *Electrochimica Acta* 55 (2010) 5123–5128.

[95] M. V. Bracamonte, M. Melchionna, A. Giuliani, L. Nasi, C. Tavagnacco, M. Prato, P. Fornasiero, H₂O₂ sensing enhancement by mutual integration of single walled carbon nanohorns with metal oxide catalysts: The CeO₂ case, *Sensors and Actuators B* 239 (2017) 923–932.

[96] Z. Yuzhong, W. Mingzhu, H. Lei, Fabrication of a Sensitive Electrochemical Biosensor for Detection of DNA Hybridization Based on Gold Nanoparticles/ CuO Nanospindles Modified Glassy Carbon Electrode, *Chin. J. Chem.* 30 (2012) 167–172.

[97] P. R. Solanki, A. Kaushik, P.M. Chavhan, S.N. Maheshwari, B.D. Malhotra, Nanostructured zirconium oxide based genosensor for Escherichia coli detection, *Electrochemistry Communications* 11 (2009) 2272–2277.

- 1
2
3 [98] M. Tak, V. Gupta , M. Tomar, Flower-like ZnO nanostructure based electrochemical DNA
4 biosensor for bacterial meningitis detection, *Biosensors and Bioelectronics* 59 (2014) 200–207.
5
6 [99] M. K. Patel, M. A. Ali, V. V. Agrawal, Z. A. Ansari, S. G. Ansari, B. D. Malhotra,
7 Nanostructured magnesium oxide biosensing platform for cholera detection, *Applied Physics*
8 *Letters* 102 (2013) 144106.
9
10 [100] B. Sahin, M. Alomari, T. Kaya. Hydration Detection through use of artificial sweat in doped-
11 and partially-doped nanostructured CuO films, *Ceramics International* 41 (2015) 8002–8007 .
12
13 [101] B. Sahin, T. Kaya, Highly improved hydration level sensing properties of Copper Oxide films
14 with Sodium and Potassium doping, *Applied Surface Science* 362 (2016) 532-537.
15
16 [102] A. Roychoudhury, S. Basu, S. K. Jha, Dopamine biosensor based on surface functionalized
17 nanostructured nickel oxide platform *Biosensors and Bioelectronics*
18 (dx.doi.org/10.1016/j.bios.2015.11.061).
19
20 [103] S. Azzouzi, L. Rotariu, A. M. Benito, W. K. Maser , M. B. Ali, C. Bala, A novel amperometric
21 biosensor based on gold nanoparticles anchored on reduced graphene oxide for sensitive detection
22 of L-lactate tumor biomarker, *Biosensors and Bioelectronics* 69 (2015) 280–286.
23
24
25
26
27
28
29
30
31
32
33
34
35
36
37
38
39
40
41
42
43
44
45
46
47
48
49
50
51
52
53
54
55
56
57
58
59
60

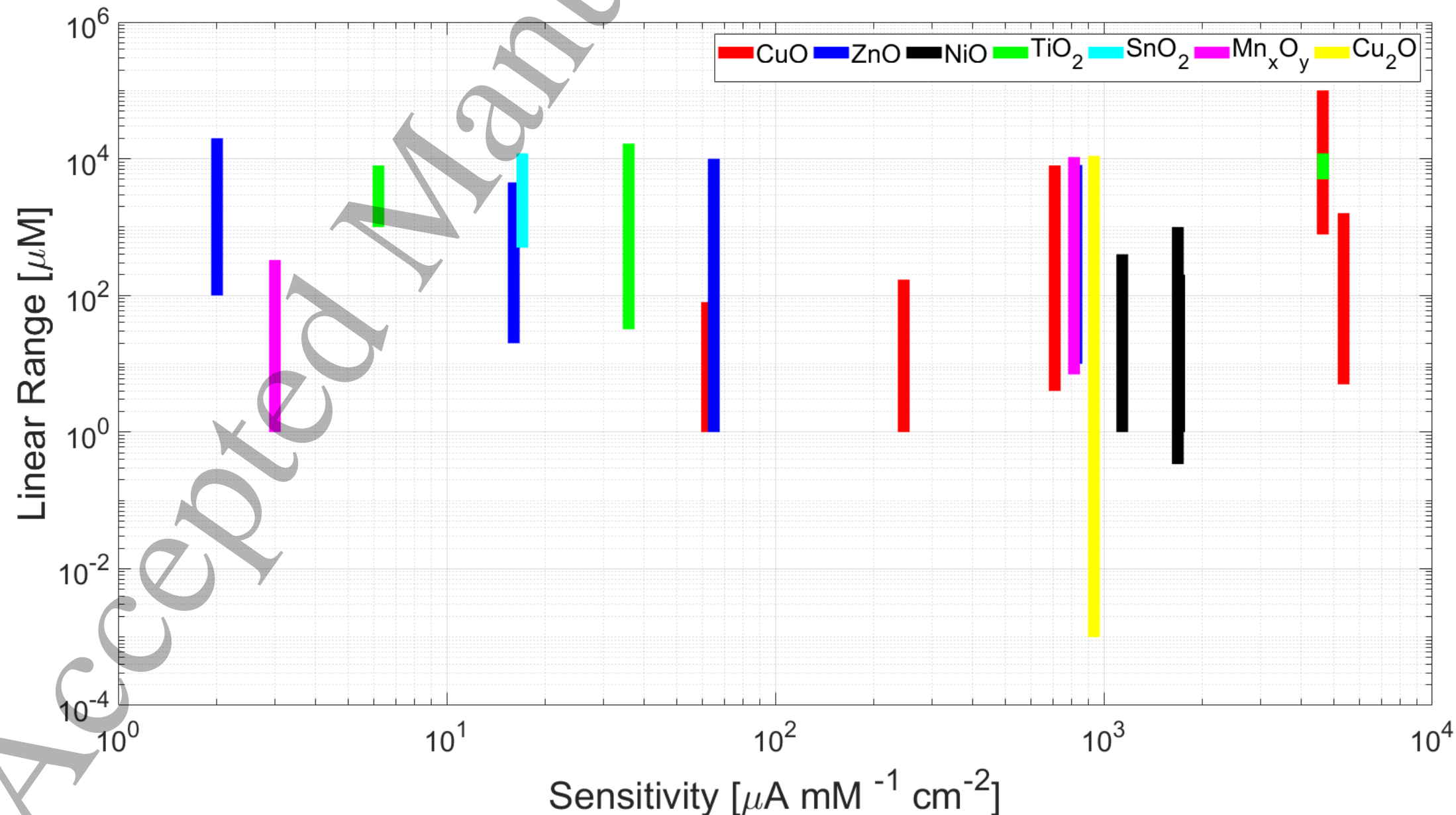


Figure 1: Glucose sensors that were listed in Table 1 were compiled by their linear range and the sensitivity. Each vertical line represents the linear range at a particular sensitivity that was reported for that particular work.

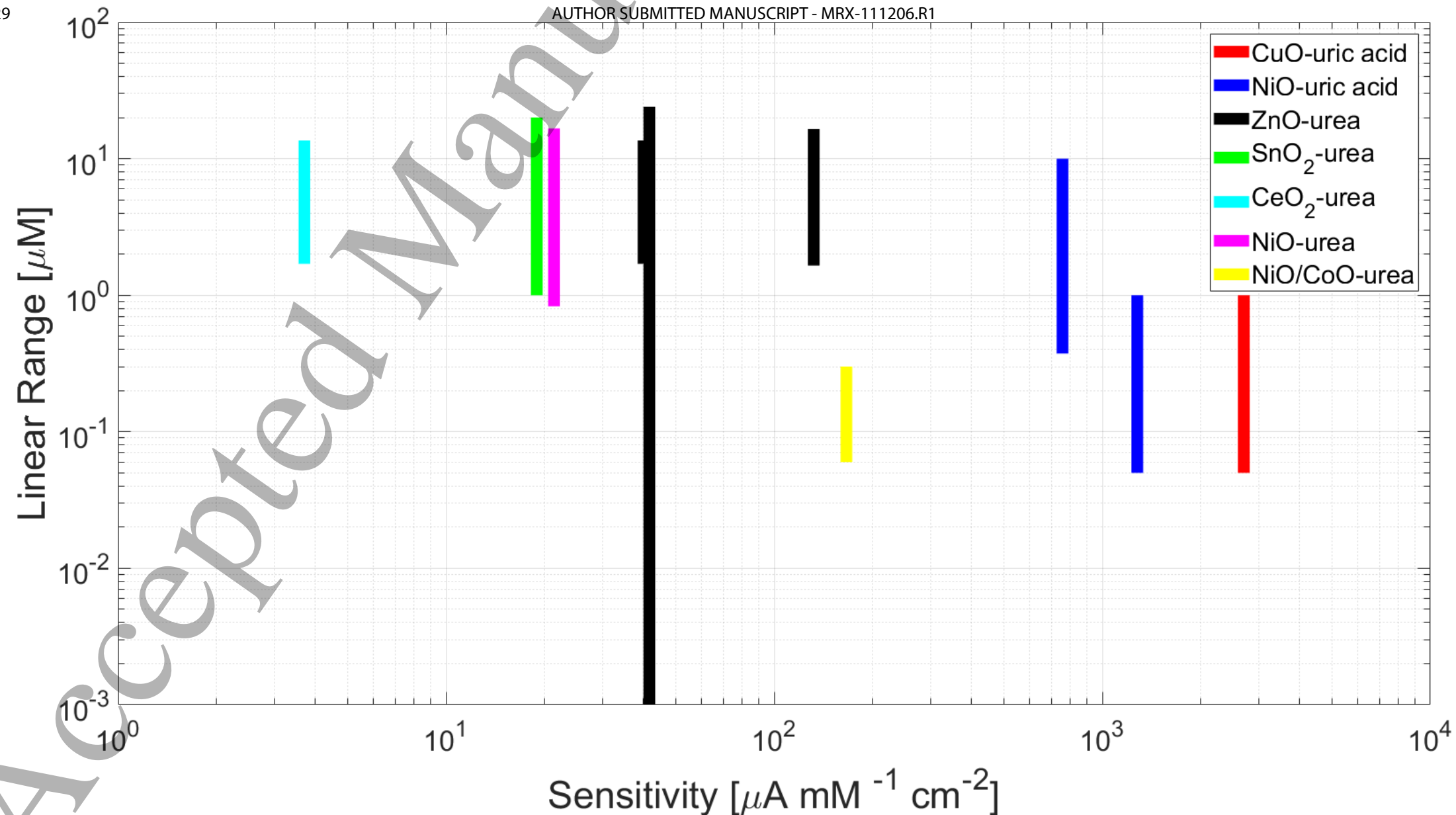


Figure 2: Urea and uric acid sensors that were listed in Table 2 were compiled by their linear range and the sensitivity. Each vertical line represents the linear range at a particular sensitivity that was reported for that particular work.

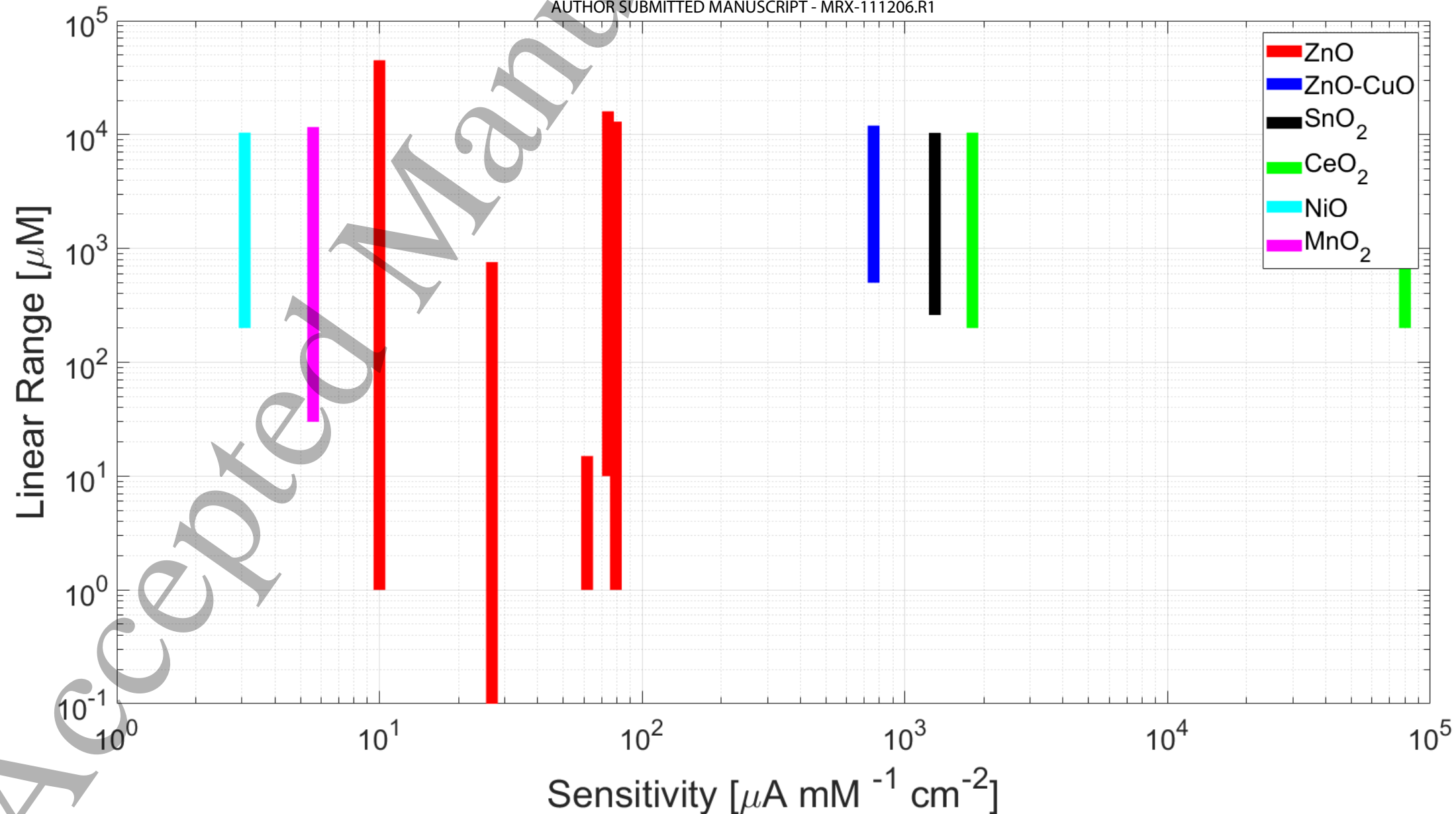


Figure 3: Cholesterol sensors that were listed in Table 3 were compiled by their linear range and the sensitivity. Each vertical line represents the linear range at a particular sensitivity that was reported for that particular work.

Structure Name	Type	Detection Range	Limit of Detection (LOD)(μM)	Michaelis–Menten Constant (K_{Mapp}) (mM)	Sensitivity value ($\mu\text{A mM}^{-1}\text{cm}^{-2}$)	Stability Duration (Day)	Stability RSD (%)	Medium	Human Serum	References
CuO	Chrysanthemum-like, candock-like, and dandelion-like	0.005 – 1.6 mM (for dandelion-like)	1.2 (for dandelion-like)		5368 (for dandelion-like)	30	3.5	NaOH	Yes	[38]
CuO	Nanospindles	1.0 - 80 μM	1		62			Phosphate buffer solution (PBS)	No	[39]
CuO	Leaf like	1.0 - 170 μM	0.91	0.29	246	90	3.28	PBS	Yes	[40]
CuO	Nanorods and flowers like	4 μM to 8 mM	4		709 (Flowers like) 371 (Nanorods)			NaOH	No	[41]
CuO	Rose like	0.78 - 100 mM	390		4640	42		PBS	No	[42]
Cu ₂ O	Shuriken-like	0.01 μM - 11.0 mM	0.035		933	80	2.7	NaOH	Yes	[43]
ZnO	Nanocombs	0.02 – 4.5 mM	20	2.19	15.33			PBS	No	[44]
ZnO	Nanorods, nanoplates	0.1 to 9 mM	1.94	3.12	1.94			PBS	No	[45]
ZnO	rod, powder, particle, cube, rock candy-like, sheet, sphere, brain-like, groundnut-like and pussy willow like	1 to 10 mM	820		64.29 (for spherical)	30	0.39	PBS	No	[46]
ZnO	Three-dimensional hierarchical	1.0 - 20 mM	20		1.4	15	5.3	PBS	Yes	[47]
ZnO	Hexagonal prisms	0.01 to 8.1mM	0.28		824.34	30	1.32	KOH	Yes	[48]
ZnO	Sputtered electrodes	0.6 μM to 11 mM*	6 μM *		14.50			PBS	Yes	[49]
TiO ₂	Nanocluster	0.032 mM – 1.67 mM	4.8	0.81	35.80		5.6	PBS	No	[50]
TiO ₂	TiO ₂ - GR nanocomposite	1 mM – 8 mM			6.2		5.6	PBS	No	[51]
TiO ₂	Nanotube arrays	1 – 12 mM	0.60		4651.0	90	8	NaOH	Yes	[52]
NiO	3D porous nanosheets	Up to 10 mM	0.90		36.13	14	6	NaOH	No	[53]
NiO	Decorated multi-walled carbon nanotubes	1 - 200 μM Up to 9 mM	0.011 31		1696 122.15	21	3.5	NaOH	Yes	[54]
NiO	Nanosheets	1 μM - 0.4 mM			1138	10	3.8	NaOH	No	[55]

NiO	Thin film	0 - 1.0 mM	0.34		1680	61	2.37	NaOH	Yes	[56]
SnO ₂	Nanostructured	0.5–12 mM.			16.90	10	10	PBS	No	[57]
CeO ₂	Nanoporous	1.39 - 8.33 mM*		1.01		70		PBS	No	[58]
MnO _x	Nanorod	0.007 - 10.6 mM	2.7		811.8	36	5.5	NaOH	Yes	[59]
Mn ₃ O ₄	Nanostructures	1.0 - 329.5 μM	0.50		2.6		5.4	NaOH	No	[60]

Table 1: Representative glucose sensors implemented using nanostructured metal oxides.

Structure Name	Type	Detection Range	Limit of Detection (LOD)(μM)	Michaelis–Menten Constant (KMapp) (mM)	Sensitivity value (μA mM ⁻¹ cm ⁻²)	Stability Duration (Day)	Stability RSD (%)	Medium	Human Serum	References
ZnO	Nanorods	0.001 - 24.0 mM	10.0	0.3280	41.64	14	2	PBS	No	[67]
ZnO	Flower-like	1.65 - 16.50 mM	7590	0.190	131.98	84	1.2	PBS	Yes	[68]
ZnO	Nanostructure	1.7 to 13.6 mM*	2300*	1.02*	40 *			PBS	No	[69]
SnO ₂	Thin film	1 - 20 mM	600		18.90			PBS	No	[70]
CeO ₂	Thin film	1.7 to 13.6 mM*	16.7*	1.04*	3.7*	180 *		PBS	No	[71]
NiO	Nanostructure	0.83 – 16.65 mM	880	0.34*	21.33	140		PBS	No	[72]
Nickel/cobalt oxide	3D graphene nanocomposite	0.06 mM – 0.30 mM*	5 mM*		166*			NaOH	No	[73]
NiO	Nanostructure	0.374 mM-10.0 mM.	0.005		756.26			NaOH	No	[74]
NiO	Thin film	0.05 mM - 1.0mM	110	0.17	1278.48	120		PBS	Yes	[75]
CuO	Thin film	0.05 - 1.0 mM.		0.12	2700	98		PBS	Yes	[76]

* Original units (mg/dL) were converted to molarity using the molar mass of glucose (180.156 g/mol).

Table 2: Representative urea and uric acid sensors implemented using nanostructured metal oxides.

* Original units (mg/dL) were converted to molarity using the molar mass of urea (60.056 g/mol).

Structure Name	Type	Detection Range	Limit of Detection (LOD) (μM)	Michaelis-Menten Constant (K_{Mapp}) (mM)	Sensitivity Value ($\mu\text{A mM}^{-1}\text{cm}^{-2}$)	Stability Duration (Day)	Stability RSD (%)	Stability Retention (%)	Medium	Human Serum	References
ZnO	Nanorods	0.01-16 mM	0.0015	0.16	74.10	45		95.0	PBS	No	[77]
ZnO	Flower-shaped	1.0 - 15.0 μM	0.012	2.57	61.7	32		83.7	PBS	No	[78]
ZnO	Nanotube	1 μM - 13 mM	0.0005		79.40	60		93	PBS	Yes	[79]
ZnO	FET	0.001 - 45mM	50		10	30		95	PBS	Yes	[80]
ZnO	Nanorods	0.1 - 759.3 μM	0.03	1.84	26.8	90		90	PBS	No	[81]
CuO-ZnO	Composite matrix	0.5-12 mM		1.8	760	98	1.4		PBS	Yes	[82]
SnO ₂	Nanobicomposite	0.26 – 10.36 mM	129.3*	3.8	1300*	56		90	PBS	No	[83]
CeO ₂	Nanocomposite	0.2 – 10.4 mM*	129.3*	0.09*	1807*	70		65	PBS	No	[84]
CeO ₂	Nano-structured	0.2 – 10.4 mM*	258.6*	2.08	80000*				PBS	No	[85]
NiO	Nanostructured	0.2 – 10.4 mM*	1128*	0.67	3.07*				NaOH	No	[86]
MnO ₂	Nanorods	0.03 - 11.66 mM	2.07		5.59	90		65	NaOH	No	[87]

Table 3: Representative cholesterol sensors implemented using metal oxides.

* Original units (mg/dL) were converted to molarity using the molar mass of cholesterol (386.65 g/mol).